Structural network efficiency is associated with cognitive impairment in small-vessel disease

OPEN

Andrew J. Lawrence, PhD
Ai Wern Chung, PhD
Robin G. Morris, PhD
Hugh S. Markus, FRCP*
Thomas R. Barrick, PhD*

Correspondence to Dr. Lawrence: alawrenc@sgul.ac.uk

ABSTRACT

Objective: To characterize brain network connectivity impairment in cerebral small-vessel disease (SVD) and its relationship with MRI disease markers and cognitive impairment.

Methods: A cross-sectional design applied graph-based efficiency analysis to deterministic diffusion tensor tractography data from 115 patients with lacunar infarction and leukoaraiosis and 50 healthy individuals. Structural connectivity was estimated between 90 cortical and subcortical brain regions and efficiency measures of resulting graphs were analyzed. Networks were compared between SVD and control groups, and associations between efficiency measures, conventional MRI disease markers, and cognitive function were tested.

Results: Brain diffusion tensor tractography network connectivity was significantly reduced in SVD: networks were less dense, connection weights were lower, and measures of network efficiency were significantly disrupted. The degree of brain network disruption was associated with MRI measures of disease severity and cognitive function. In multiple regression models controlling for confounding variables, associations with cognition were stronger for network measures than other MRI measures including conventional diffusion tensor imaging measures. A total mediation effect was observed for the association between fractional anisotropy and mean diffusivity measures and executive function and processing speed.

Conclusions: Brain network connectivity in SVD is disturbed, this disturbance is related to disease severity, and within a mediation framework fully or partly explains previously observed associations between MRI measures and SVD-related cognitive dysfunction. These cross-sectional results highlight the importance of network disruption in SVD and provide support for network measures as a disease marker in treatment studies. *Neurology*® 2014;83:304–311

GLOSSARY

AAL = Automated Anatomical Labeling; **DTI** = diffusion tensor imaging; **DTT** = diffusion tensor tractography; **EF** = executive function; $\mathbf{E_{Global}}$ = global efficiency; $\mathbf{E_{Local}}$ = local efficiency; $\mathbf{E_{Nodal}}$ = nodal efficiency; **FA** = fractional anisotropy; **FLIRT** = FMRIB's Linear Image Registration Tool; **FSL** = FMRIB Software Library; **GENIE** = St George's Neuropsychology and Imaging in Elderly; **MD** = mean diffusivity; **MLR** = multiple linear regression; **NART** = National Adult Reading Test; **NBS** = network-based statistic; **NBV** = normalized brain volume; **PS** = processing speed; **SCANS** = St George's Cognition and Neuroimaging in Stroke Study; **SVD** = small-vessel disease; **WMLL** = white matter lesion load.

Cerebral small-vessel disease (SVD) is the major cause of vascular cognitive impairment, with characteristic early deficits in executive function (EF) and processing speed (PS).[1] The pathophysiologic basis for these deficits remains incompletely understood. Diffusion tensor imaging (DTI) suggests diffuse white matter ultrastructural damage is important in cognitive impairment, while lacunar infarcts, white matter hyperintensities, and brain atrophy have also been implicated.

Cognitive functions depend on efficient functioning of distributed brain networks connected by white matter tracts. SVD pathologies could disrupt these connections, impairing network functioning and cognition via a disconnection "syndrome."[2] A better understanding of how

Editorial, page 296

Supplemental data at Neurology.org

*These authors contributed equally to this work.

From the Stroke & Dementia Research Centre (A.J.L., A.W.C., T.R.B.), St George's University of London; Department of Psychology (R.G.M.), Institute of Psychiatry, King's College London; and Clinical Neurosciences (H.S.M.), University of Cambridge, UK.

Go to Neurology.org for full disclosures. Funding information and disclosures deemed relevant by the authors, if any, are provided at the end of the article.

these processes cause cognitive impairment is important in developing evidence-based treatment strategies.

Graph analysis allows the quantitative analysis of network organization,[3,4] describing the connections of the brain as a collection of nodes (brain regions) that communicate by connecting edges (white matter tracts) defined by diffusion tensor tractography (DTT). Graph-based measures of the organizational characteristics of structural brain networks are disrupted in disease,[5–7] particularly those with white matter pathology.[8,9] Network measures (appendix e-1 on the *Neurology*® Web site at Neurology.org) can assess how information is globally integrated, or the extent to which the network forms local clusters of interconnected nodes supporting specialized information processing modules.

We applied graph analysis to DTT from patients with SVD. We hypothesized that SVD would be characterized by widespread network disruption, which would be associated with diffuse white matter damage detectable on DTI. We further hypothesized that network disruption would be associated with cognitive dysfunction.

METHODS

Standard protocol approvals, registrations, and patient consents. Study protocols were approved by a local research ethics committee. Participants provided prior written informed consent.

Study design. This was a cross-sectional study correlating cognitive testing with MRI parameters in patients with SVD.

Participants. Data are reported from 115 patients with symptomatic SVD (SVD group; 39 women [33.6%]; mean age 70.2 ± 9.7 years) and 50 healthy controls (21 women [42%]; mean age 70.2 ± 9.3 years). The patients with SVD were participating in a longitudinal study investigating the relationship between MRI markers and cognition in SVD (the St George's Cognition and Neuroimaging in Stroke Study [SCANS]). Patients were recruited between March 2007 and October 2010 from the inpatient and outpatient stroke services of 3 hospitals covering a geographically contiguous area of South London (St George's, King's College, and St Thomas' Hospitals). All offered a comprehensive stroke service. SVD was defined as a clinical lacunar stroke syndrome, with an anatomically appropriate lacunar infarct on MRI, in addition to confluent leukoaraiosis (Fazekas grade 2 or higher).[10]

Exclusion criteria included any stroke mechanism other than SVD, including extra- or intracranial large artery stenosis >50%, cardioembolic source, nonlacunar subcortical infarcts (>1.5 cm in diameter), or cortical infarcts, and a history of major neurologic or psychiatric disorders (with the exception of depression).[11]

Controls were community-based, stroke-free individuals recruited to the St George's Neuropsychology and Imaging in Elderly (GENIE) Study.[12] Exclusion criteria included history of major neurologic or psychiatric disorders. Sample size in SCANS was decided based on the number required to detect a correlation of 0.4 with 90% power at $\alpha = 0.005$. One hundred eighty patients were screened, 137 consented, and 121 completed the assessment protocol.[13] Six patients were excluded because of inadequate MRI data (acquisition error, or failure of the analysis pipeline).

Cognitive measures. A trained neuropsychologist administered neuropsychological tests to assess premorbid National Adult Reading Test (NART) IQ and 4 broad cognitive domains: EF, PS, working memory, and episodic (long-term) memory. Baseline results have been previously published,[11] and further details are provided in appendix e-2.

Image acquisition. Images were acquired at St George's University of London using a 1.5T Signa HDxt MRI system (General Electric, Milwaukee, WI) with a maximum gradient amplitude of 33 mTm^{-1} and a proprietary head coil within 45 minutes. The following whole-brain sequences were acquired: axial fluid-attenuated inversion recovery, coronal spoiled gradient recalled echo 3-dimensional T1-weighted, axial single shot diffusion-weighted spin echo planar imaging with isotropic voxels (2.5 mm^3), and 25 noncollinear diffusion gradient directions at $b = 1{,}000\ s \cdot mm^{-2}$ in positive and negative gradient directions. Full acquisition details have been previously published.[11]

Conventional markers of MRI pathology. The following markers were analyzed for patients and controls:

1. Brain volume: Normalized and nonnormalized brain parenchyma volumes were automatically calculated on T1-weighted images using SIENAX (FMRIB Software Library, FSL v4.1; http://www.fmrib.ox.ac.uk/fsl/).[14] Normalized brain volume (NBV) is an estimate of brain parenchyma volume adjusted for skull size and thus a measure of brain atrophy in cross-sectional data.[14]
2. White matter lesions: A trained rater delineated hyperintense white matter regions on fluid-attenuated inversion recovery images using the semiautomated DISPUNC program (David Plummer, University College, London).[15] Lesions ≥2 mm in diameter were delineated to create whole-brain lesion maps. White matter lesion load (WMLL) was calculated as a percentage of nonnormalized brain volume.
3. Lacunar infarcts: Lacunar infarcts were counted on T1-weighted images by an expert rater.

Diffusion MRI analysis. Diffusion-weighted images were corrected for eddy current distortions using FSL Linear Image Registration Tool (FLIRT; FSL v4.1).[16] Gradient cross terms were removed,[17] and DTI calculated.[18] Histogram analysis was used to provide median values for fractional anisotropy (FA) and mean diffusivity (MD) in normal-appearing white matter.[11]

Diffusion tensor tractography. Whole-brain deterministic DTT[19] was seeded from a grid at super-resolution[20] (0.5 mm^3) using in-house software. Streamlines were terminated at an angle, $\theta \geq 40°$ between principal eigenvectors, or $FA < 0.2$.

Network nodes. Nodes were defined using the Automated Anatomical Labeling (AAL) atlas,[21] a widely used atlas in network studies.[6–9,22] The 90 AAL regions of interest were transformed into subject space. Each subject's T1-weighted image was registered to DTI space ($b = 0\ s \cdot mm^{-2}$ map) using FLIRT. A symmetric diffeomorphic nonlinear transformation was computed between the T1-weighted image and Montreal Neurological Institute space (Colin27 image provided with MRIcro, www.mricro.com) using Advanced Normalization Tools.[23] Optimal normalization

parameters were applied.[24] These transformations were combined to transform the AAL atlas image to each subject's DTI space.

Network edges. Connectivity weights were ascribed to edges to capture information about connection strength. Edge weights (w_{ij}) were modified from Hagmann et al.[3] based on the lengths (in mm), l of the set of N streamlines with end points terminating in each pair of nodes i and j,

$$w_{ij} = \frac{1}{2}\sum_{m=0}^{N}\frac{1}{l_m}$$

This includes a scaling factor to correct for the number of seeds per millimeter. Connectivity distance d_{ij} was calculated as:

$$d_{ij} = \frac{1}{w_{ij}}.$$

This weighting technique has the benefit of simple interpretation; i.e., w_{ij} represents the seeding-corrected number of unique streamlines passing between i and j. Networks were thresholded at $w_{ij} = 1$ to minimize noise-related false-positives.

Network analysis. Network efficiency was computed using the Brain Connectivity Toolbox[4] (www.brain-connectivity-toolbox.net). Efficiency between 2 regions is defined as the inverse length of the shortest path between them, reflecting the ease with which regions communicate in parallel. Efficiency analysis is suitable for networks with disconnected nodes[25] (i.e., for disconnected nodes [$E = \infty^{-1} = 0$]), which were common in both controls (44%) and patients with SVD (50%; $p = 0.6255$). Formulae are presented in appendix e-1.

Entire network analysis. Summary measures of network properties of the whole-brain network were calculated. Global efficiency (E_{Global}) reflects integration over the whole network and is estimated by averaging efficiency for all node pairs. The average local efficiency (E_{Local}) measures clustering and specialization within a network and is calculated from the efficiency of the connections between first-degree neighbors of each node. To confirm previous findings of small-worlded topology in structural brain networks, normalized "small-world" parameters, N (E_{Global}) and N (E_{Local}), were computed from E_{Global} and E_{Local} dividing each by average parameters derived from 500 randomly rewired null-model networks.[26]

Regional network analysis. Two complementary approaches were followed to explore the location of network disruption. Nodal efficiency (E_{Nodal}) was computed, which reflects the integration of each node with the remainder of the network. E_{Nodal} measures were compared between SVD and control groups to identify regional differences (appendix e-3). Second, the network-based statistic[27] (NBS) was applied to the network edge weights. A 2-sample t statistic was applied to weights for each edge, and those with $t > 3.4$ (corresponding to $p < 0.0005$, uncorrected) were systematically searched for connected edges showing the same effect. Permutation testing (n = 10,000) was used to provide multiple-comparisons correction using the family-wise error ($p < 0.01$). The NBS identifies the subnetwork(s) of connected edges that differ the most between groups.

Statistical analysis. Statistical analysis was performed in R (www.R-project.org). Normality of continuous variables was checked, and appropriate transformations were applied to WMLL and lacune count ($\log_{10}$).

Welch independent samples t tests were used to compare SVD and control demographics and network measures. Within the SVD group Pearson correlation coefficients were used to test associations between network measures and other MRI markers associated with SVD. Tests were adjusted for multiple comparisons.[28]

For analyses involving MRI measures and cognitive variables, multiple linear regression (MLR) models were used, controlling for variables known to affect cognitive function (age, sex, and NART IQ), henceforth termed *confounders*. To identify shared prediction between network measures and MRI measures, pairwise MLR (with control variables) was conducted. Finally, estimates of direct and indirect causal mediation effects were obtained from MLR models.[29] Variance inflation factors were calculated for terms in all MLR models and indicated no significant multicollinearity (<4).

Table 1 MRI and global network differences between healthy controls and patients with SVD

	Control group (n = 50)	SVD group (n = 115)	Test statistic[a]	p Value
Conventional MRI measures				
WMLL[b]	0.84 (1.2)	3.1 (2.6)	$t_{128.2} = -9.0$	<0.0001
NBV, mL	1,338.3 (85.2)	1,295.2 (93.1)	$t_{101.3} = 2.9$	0.005
Median FA (histogram)	0.33 (0.019)	0.29 (0.028)	$t_{133.9} = 10.6$	<0.0001
Median MD (histogram)[c]	0.77 (0.03)	0.80 (0.032)	$t_{97.8} = -6.5$	<0.0001
Entire network measures				
Edge density	0.12 (0.016)	0.10 (0.019)	$t_{106.5} = 6.9$	<0.0001
Vertex strength[d]	184.7 (39.62)	145.5 (41.12)	$t_{96.5} = 5.8$	<0.0001
E_{Global}	10.1 (2.15)	8.0 (2.2)	$t_{97} = 5.5$	<0.0001
E_{Local}[d]	9.8 (1.6)	8.4 (1.9)	$t_{105.2} = 4.8$	<0.0001
Normalized E_{Global}	0.87 (0.034)	0.86 (0.044)	—	—
Normalized E_{Local}[d]	2.5 (0.5)	3.4 (1.0)	—	—

Abbreviations: E_{Global} = global efficiency; E_{Local} = local efficiency; FA = fractional anisotropy; MD = mean diffusivity; NBV = normalized brain volume; SVD = small-vessel disease; WMLL = white matter lesion load.
Presented are mean (SD) group descriptives and t tests for significant differences for MRI, diffusion tensor imaging, and network measures. Formulae for network measures are provided in appendix e-1.
[a] Welch t test for unequal population variances (subscript adjusted degrees of freedom).
[b] Test statistic derived from variance stabilized ($\log_{10}$) transformed data.
[c] MD units: $mm^2 \cdot s^{-1}$ ($\times 10^{-3}$).
[d] Mean average across nodes.

RESULTS SVD and control groups were well matched for age ($p = 0.9$) and sex ($p = 0.4$). Cognitive function was impaired in SVD for EF ($p < 0.0001$) and PS ($p < 0.0001$) indices, but not for working memory ($p = 0.12$) or long-term (episodic) memory ($p = 0.9$). Further descriptives are presented in table e-1.

Entire network analysis. All constructed structural brain networks were sparse (approximately 10% dense) and met criteria for "small-worldedness" (normalized $E_{Global} < 1$, normalized $E_{Local} >> 1$). SVD networks were less dense, with lower weighted edges and reduced E_{Global} and E_{Local} relative to controls (table 1).

Regional network analysis. E_{Nodal} was compared between SVD and controls for each node in the

network, and 85 of 90 nodes (94%) had significantly reduced efficiency in SVD (appendix e-3; figures e-1, e-2, and e-3).

NBS analysis identified a single subnetwork ($p < 0.001$) with maximally impaired connectivity in SVD. This network is widely distributed (figure 1), involving 29 edges between 27 unique nodes (tables e-2, e-3, and e-4). The white matter pathway anatomy is described in appendix e-4. Interhemispheric connections (table e-2) were overrepresented, comprising 10 of 29 (34.4%) of the impaired network but only 68 of 443 (15.3%) of all connections (on average; $p < 0.0067$). These included all major subdivisions of the corpus callosum[30] and intersected centrum semiovale white matter lesions. Connections of the inferior and superior frontal gyri were also disproportionately impaired (15/29, $p < 0.01$). Impaired association tracts (n = 10, table e-3) predominantly involved prefrontal cortex, including fronto-frontal connections of the superior frontal gyrus and pathways between inferior frontal cortex and parietal and temporal regions. Remaining tracts (n = 9, table e-4) involved frontal and precuneus pathways to basal ganglia, limbic, and insular regions. Several white matter pathways were identified including the left frontal U-fibers, bilateral aslant tract, bilateral inferior fronto-occipital fasciculus, right frontoinsular system, and right parahippocampal cingulum. Minimal overlap was found between these tract locations and regions frequently affected by white matter lesions.

Network measures and MRI markers. In the SVD group, network measures correlated with MRI measures such that more severe MRI markers of SVD were associated with network disruption (table 2). Strongest associations were seen for FA and MD DTI measures, but all tested associations were significant.

Network measures and cognition. Multiple regression models controlling for confounders (age, sex, NART IQ) were constructed to predict cognitive function indices from all network parameters (E_{Global}, E_{Local}).

Figure 1 Subnetwork identified as impaired in patients with small-vessel disease relative to controls

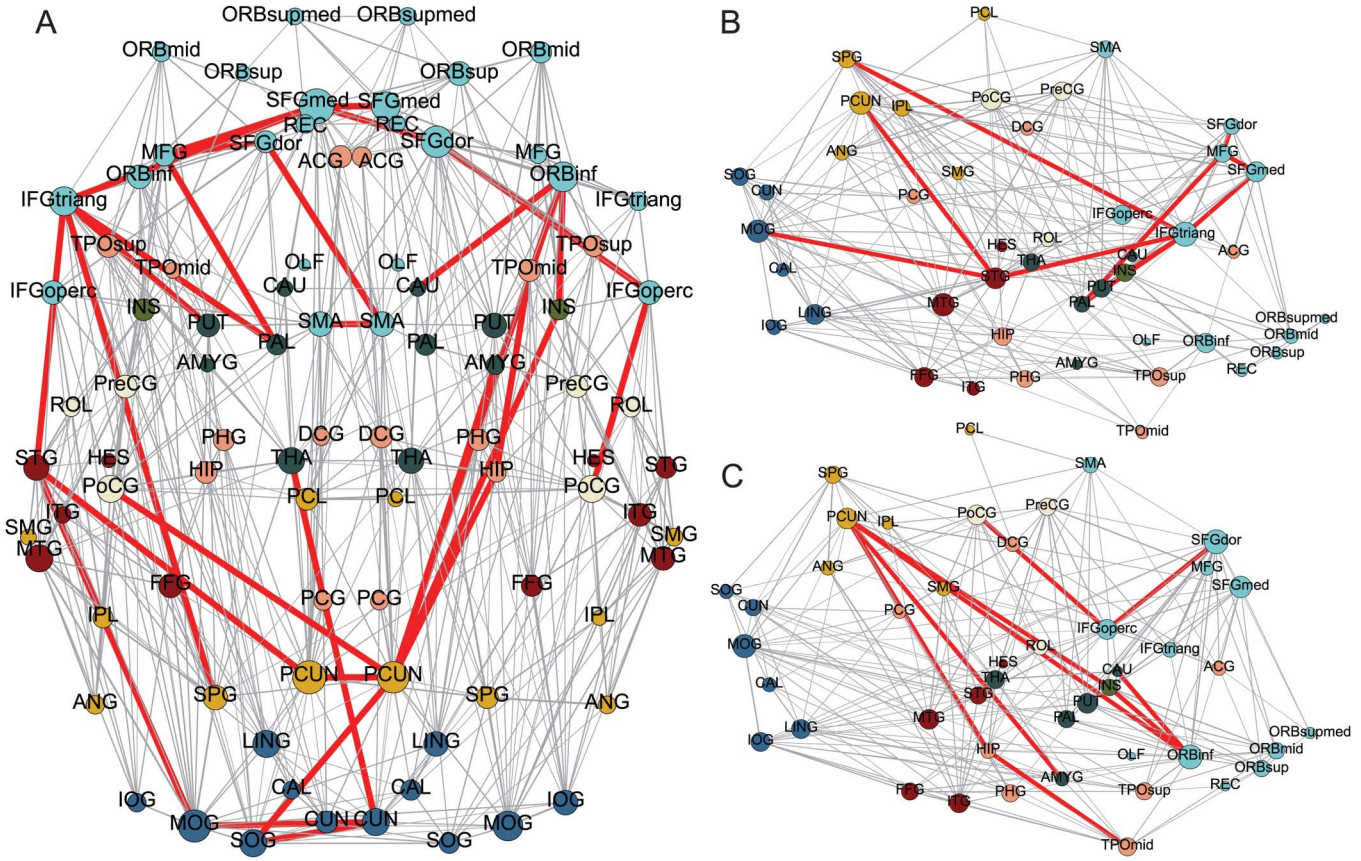

Projections of an example brain network taken from a randomly selected control subject (gray edges). (A) Whole-brain axial view. (B) Left hemisphere sagittal view. (C) Right hemisphere sagittal view. The network-based statistic significant subnetwork of impaired connections is overlaid in red ($p < 0.001$ adjusted, threshold of $t = 3.4$) (see appendix e-3; tables e-2, e-3, and e-4). Nodes are displayed as circles located at region of interest centers of gravity, with circle size scaled corresponding to degree. Node colors group Automated Anatomical Labeling regions according to brain macro-regions: light blue = frontal lobe cortex; blue-gray = subcortical regions; coral = limbic and paralimbic regions; dark red = temporal lobe cortex; yellow = parietal lobe cortex; cream = motor cortex; dark blue = occipital cortex. See appendix e-5 for key.

Table 2 Global network properties in the SVD group are associated with MRI measures of SVD

	WMLL	Lacunes	NBV	Median FA	Median MD
Edge density	−0.61	−0.47	0.54	0.82	−0.79
Vertex strength	−0.56	−0.41	0.49	0.79	−0.74
E_{Global}	−0.57	−0.42	0.50	0.78	−0.73
E_{Local}	−0.53	−0.39	0.42	0.76	−0.72

Abbreviations: E_{Global} = global efficiency; E_{Local} = local efficiency; FA = fractional anisotropy; MD = mean diffusivity; NBV = normalized brain volume; SVD = small-vessel disease; WMLL = white matter lesion load.
Pearson correlation coefficients are presented. All coefficients were significantly different from zero ($p < 0.05$ Holm-Bonferroni corrected). Formulae for network measures are provided in appendix e-1.

All regression coefficients were significant ($p < 0.05$, uncorrected) such that network disruption was associated with worse cognitive performance. Associations were strongest for PS (E_{Global}: $\beta = 0.39$, $p < 0.0001$; E_{Local}: $\beta = 0.365$, $p < 0.0001$) followed by EF (E_{Global}: $\beta = 0.33$, $p < 0.0001$; E_{Local}: $\beta = 0.29$, $p = 0.0001$). Weaker associations were seen for working memory (E_{Global}: $\beta = 0.235$, $p = 0.009$; E_{Local}: $\beta = 0.197$, $p = 0.024$) and long-term memory (E_{Global}: $\beta = 0.26$, $p = 0.003$; E_{Local}: $\beta = 0.279$, $p = 0.001$). Given a priori interest in EF and PS cognitive indices in SVD[31] and the findings above, we restricted subsequent analyses to these indices. Because E_{Global} and E_{Local} are highly correlated, subsequent analysis is presented for E_{Global} as a marker of network disruption. Appendix e-3 and figure e-2 present linear models predicting cognitive indices EF and PS from E_{Nodal} values. Most nodes (83/90) were significantly associated with cognition at magnitudes comparable to E_{Global} and E_{Local}.

Table 3 Multiple regression models of MRI measures before and after controlling for network global efficiency

	Model 1	Model 2: MRI	Model 2: E_{Global}
Processing speed			
WMLL	−0.226 (0.008)	−0.014 (0.9)	0.381 (0.0002)
Lacune count	−0.328 (<0.0001)	−0.199 (0.019)	0.277 (0.003)
NBV	0.371 (<0.0001)	0.244 (0.006)	0.262 (0.005)
Median FA	0.315 (0.0006)	−0.014 (0.9)	0.400 (0.003)
Median MD	−0.280 (0.001)	−0.002 (0.99)	0.389 (0.001)
Executive function			
WMLL	−0.096 (0.2)	0.130 (0.14)	0.406 (<0.0001)
Lacune count	−0.260 (0.0004)	−0.139 (0.086)	0.250 (0.005)
NBV	0.296 (<0.0001)	0.182 (0.03)	0.233 (0.008)
Median FA	0.247 (0.003)	−0.077 (0.6)	0.387 (0.002)
Median MD	−0.215 (0.008)	0.058 (0.6)	0.371 (0.001)

Abbreviations: E_{Global} = global efficiency; FA = fractional anisotropy; MD = mean diffusivity; NBV = normalized brain volume; WMLL = white matter lesion load.
Displayed are standardized regression coefficients (β) (with parenthetical *p* values) for models comparing conventional MRI measures with E_{Global} as predictors of cognitive function (processing speed, executive function) in the small-vessel disease group. Model 1 shows coefficients for each MRI measure in a regression controlling for confounder variables (age, sex, National Adult Reading Test IQ). Model 2: MRI shows the same coefficient in a regression model that also controls for E_{Global}. Model 2: E_{Global} shows the coefficient for the E_{Global} network measure from this model.

Predicting cognitive impairment: Multiple regression models. Table 3 shows the effects of including E_{Global} in multiple regression models to predict SVD-related cognitive function (EF, PS) from the conventional MRI markers: WMLL, lacune count, NBV, and median FA and MD. E_{Global} remained significant when controlling for the MRI markers (table 3, column 4); however, the effects of controlling markers for E_{Global} varied. For WMLL, FA, and MD measures, the unique variance explained in the cognitive measure is reduced (table 3), and in each case, the MRI marker is no longer independently significant. For NBV and lacune count, the decrease in regression coefficient is smaller, and a significant independent effect remains. Figure 2 displays path diagrams for FA and MD measures in a causal mediation framework. Given reported associations between depression and cognitive function, all multiple regression analyses from table 3 were repeated with the Geriatric Depression Scale score added as a covariate. The largest absolute change in regression coefficient was small ($\beta = 0.025$), suggesting that depressive symptoms do not underlie the reported relationships.

DISCUSSION In this study, we used DTT and network analysis to explore the effects of SVD on the network of white matter structural connections. Compared with healthy controls, SVD networks showed evidence of widespread disruption both to global integration and localized segregation. Networks were less densely connected, with lower connection weights and reductions in both global and local efficiency. Regional analysis confirmed widespread connectivity differences throughout the brain. However, a subnetwork of the most impaired connections was identified and characterized by involvement of interhemispheric and prefrontal tracts. The former were partly explained by lesion distribution while the latter define prefrontal connections that would not have been identified by conventional MRI techniques. This impairment of prefrontal connectivity provides a potential mechanism for EF deficits observed in SVD. Measures of network disruption (E_{Global}, E_{Local}) were associated with MRI markers of SVD and cognitive function. When compared with currently used MRI markers, network global efficiency was shown to fully or partly mediate the relationship between MRI markers and cognition.

Figure 2 Diagrams showing statistical mediation of the relationship between diffusion tensor imaging measures and cognitive function by network efficiency in small-vessel disease

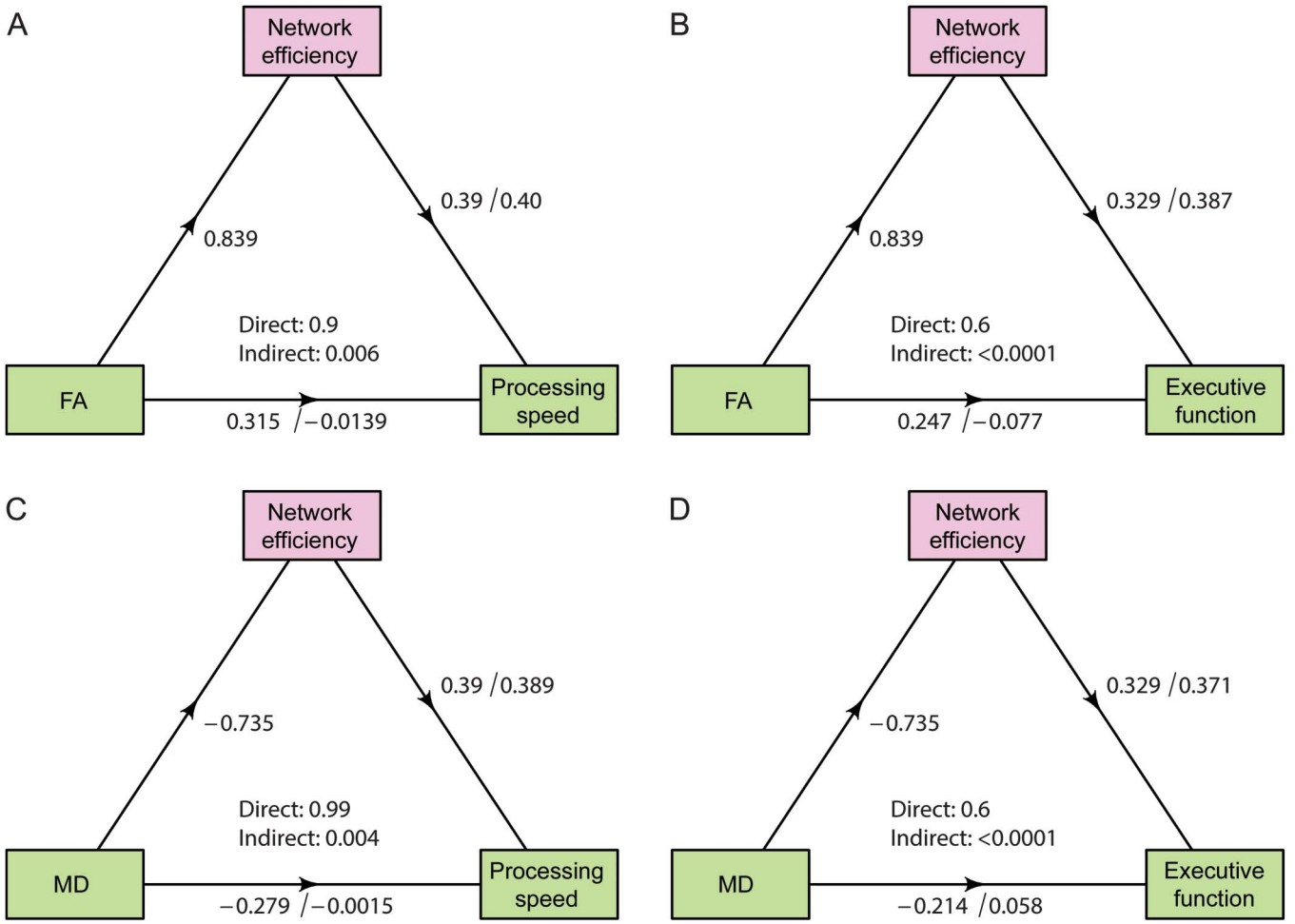

(A, B) Mediation models for the effect of fractional anisotropy (FA). (C, D) Mediation models for the effect of mean diffusivity (MD). These are then used to show models to predict processing speed (A and C) and models to predict executive function (B and D). Diagrams present the standardized regression coefficients controlling for confounders associated with each path in the model. Coefficients after the slash show path values adjusted for the mediation effect. The bootstrap statistical significance (*p* values) of the direct and indirect paths is presented in the center of each diagram.

Our findings of disrupted network measures in SVD, and their associations with cognitive function, are consistent with previous studies in multiple sclerosis,[8] diabetes,[9] and old age,[32] which all feature white matter damage. Furthermore, these disorders display impairments of information processing speed and EF, and reduced global efficiency of structural networks with the severity of disruption related to cognitive task performance. The consistency in findings across different white matter diseases suggests the importance of network integrity for cognitive function and the suitability of DTT network measures as markers for cognitive dysfunction in disorders with diffuse white matter pathology.

Expanding on previous investigations of MRI markers in SVD,[11] we tested the hypothesis that disrupted network topology mediates associations between conventional MRI measures of SVD. Our results show that, for MRI measures of diffuse white matter damage, associations with cognition are fully mediated by network disruption. In contrast, brain volume and lacunes have independent associations with cognition, although some variance is shared with network disruption. This evidence highlights the importance of network disruption as a mediating mechanism between white matter changes and cognitive dysfunction in SVD. It further suggests that network measures have potential as a marker for use in studies of cognitive impairment in SVD, although longitudinal studies are required to confirm these findings.

We studied a large, well-phenotyped sample with SVD covering a range of severity. Control subjects were well matched by demographics and are representative of the general population rather than selected for the absence of signs of ischemic change. Frequently reported techniques for network construction and analysis and widely used psychological

tasks were used. However, the study has a number of limitations.

Although cognitive testing was performed in the controls as previously published,[12] the tests used differed slightly and therefore direct comparison between SVD and controls was not possible. We have previously compared SVD patients with identical inclusion criteria with controls from the GENIE cohort and demonstrated differences in cognition, particularly in EF and information processing speed.[33]

Diffusion imaging is currently the only in vivo method for probing white matter connectivity but has limitations.[34] DTI voxels are orders of magnitude larger than axonal structure producing partial volume effects with consequences for DTT. For example, tract geometries are ambiguous through regions including white matter fiber fanning, crossing, kissing, or twisting. The deterministic DTT methods we used do not capture uncertainty in fiber orientation[35] and are incapable of resolving multiple fiber orientations within a voxel.[35] To minimize the impact of these limitations, we used DTT seeded from regions with well-defined principal diffusion directions (FA $\geq$ 0.2) and used super-resolution seeding to reduce partial volume effects.[20] Further investigation using high angular resolution diffusion-weighted MRI would allow verification of our findings with more complex tractography techniques.

We found differences between subjects with SVD and controls in several measures of structural connectivity consistent with widespread sporadic disruption of the structural network. However, networks differed in density, and inferences cannot be made regarding specific topologic aspects of the networks. This is a known disadvantage of network analysis in DTT for which there is presently no bias-free correction.[36,37] Therefore, while networks are undoubtedly less efficient in SVD, the extent to which this is related to disrupted topology or reduced network density is unclear.

The AAL atlas comprises differently sized anatomical regions that may affect obtained network properties.[38] Alternative techniques such as high-resolution random parcellation[3] may provide different results. However, it is unclear how using large numbers of equal-sized node regions that do not directly represent anatomical structures will improve study interpretation or that a higher node resolution improves reliability.[39] Using functional activations to define nodes may provide a more interpretable solution.[40]

In summary, by applying network analysis to diffusion tensor MRI, we showed that white matter network connectively was impaired in patients with symptomatic SVD, and that the degree of this disruption was related to cognitive impairment. Our data are consistent with SVD causing cognitive impairment via diffuse disruption of white matter networks. Network analysis may provide a useful disease marker to monitor the disease and study therapeutic interventions.

AUTHOR CONTRIBUTIONS

Dr. Lawrence: study concept and design, drafting and revision of manuscript, analysis and interpretation of data, acquisition of data, and statistical analysis. Dr. Chung: drafting and revision of manuscript, analysis and interpretation of data, and acquisition of data. Prof. Morris: study concept and design, drafting and revision of manuscript, analysis and interpretation of data, study supervision and coordination, obtaining funding. Prof. Markus: study concept and design, drafting and revision of manuscript, analysis and interpretation of data, study supervision and coordination, obtaining funding. Dr. Barrick: study concept and design, drafting and revision of manuscript, analysis and interpretation of data, acquisition of data, study supervision and coordination, obtaining funding.

ACKNOWLEDGMENT

The authors gratefully acknowledge the contributions of the following individuals toward this report: Dr. Bhavini Patel for help with data collection and image analysis, Dr. Thomas Willis and Dr. Poneh Adib-Samii for help with data collection, Dr. Andrew Mackinnon and Dr. Phil Rich for image analysis of lacunes and CMB, and Prof. Lalit Kalra and Prof. Tony Rudd for assistance with recruitment. The authors thank the Neuroergonomics Research Team of the University of Iowa's Department of Neurology for their Grooved Pegboard normative data, obtained in their NIH-sponsored research.

STUDY FUNDING

Study funding was provided by the Wellcome Trust (grant 081589). Recruitment to the study was supported by the English National Institute of Health Research Clinical Stroke Research Network. The article processing charge was paid by the Wellcome Trust.

DISCLOSURE

A. Lawrence is supported by a research grant from Alzheimer's Research UK (ARUK-PG2013-2). A. Chung reports no disclosures relevant to the manuscript. R. Morris serves on the consultant and advisory panel for P1 vital Limited. H. Markus is supported by an NIHR senior investigator award. T. Barrick reports no disclosures relevant to the manuscript. Go to Neurology.org for full disclosures.

Received August 23, 2013. Accepted in final form February 24, 2014.

REFERENCES

1. Pantoni L. Cerebral small vessel disease: from pathogenesis and clinical characteristics to therapeutic challenges. Lancet Neurol 2010;9:689–701.
2. O'Sullivan M, Jones DK, Summers PE, Morris RG, Williams SC, Markus HS. Evidence for cortical "disconnection" as a mechanism of age-related cognitive decline. Neurology 2001;57:632–638.
3. Hagmann P, Kurant M, Gigandet X, et al. Mapping human whole-brain structural networks with diffusion MRI. PLoS One 2007;2:e597.
4. Rubinov M, Sporns O. Complex network measures of brain connectivity: uses and interpretations. Neuroimage 2010;52:1059–1069.
5. Griffa A, Baumann PS, Thiran JP, Hagmann P. Structural connectomics in brain diseases. Neuroimage 2013;80:515–526.
6. Reijmer YD, Leemans A, Caeyenberghs K, et al. Disruption of cerebral networks and cognitive impairment in Alzheimer disease. Neurology 2013;80:1370–1377.
7. Lo CY, Wang PN, Chou KH, Wang J, He Y, Lin CP. Diffusion tensor tractography reveals abnormal topological

organization in structural cortical networks in Alzheimer's disease. J Neurosci 2010;30:16876–16885.
8. Shu N, Liu Y, Li K, et al. Diffusion tensor tractography reveals disrupted topological efficiency in white matter structural networks in multiple sclerosis. Cereb Cortex 2011;21:2565–2577.
9. Reijmer YD, Leemans A, Brundel M, Kappelle LJ, Biessels GJ; Utrecht Vascular Cognitive Impairment Study Group. Disruption of the cerebral white matter network is related to slowing of information processing speed in patients with type 2 diabetes. Diabetes 2013;62:2112–2115.
10. Fazekas F, Chawluk JB, Alavi A, Hurtig HI, Zimmerman RA. MR signal abnormalities at 1.5 T in Alzheimer's dementia and normal aging. AJR Am J Roentgenol 1987;149:351–356.
11. Lawrence AJ, Patel B, Morris RG, et al. Mechanisms of cognitive impairment in cerebral small vessel disease: multimodal MRI results from the St George's Cognition and Neuroimaging in Stroke (SCANS) Study. PLoS One 2013;8:e61014.
12. Charlton RA, Barrick TR, Markus HS, Morris RG. The relationship between episodic long-term memory and white matter integrity in normal aging. Neuropsychologia 2010;48:114–122.
13. Patel B, Lawrence AJ, Chung AW, et al. Cerebral microbleeds and cognition in patients with symptomatic small vessel disease. Stroke 2013;44:356–361.
14. Smith SM, Zhang Y, Jenkinson M, et al. Accurate, robust, and automated longitudinal and cross-sectional brain change analysis. Neuroimage 2002;17:479–489.
15. Grimaud J, Lai M, Thorpe J, et al. Quantification of MRI lesion load in multiple sclerosis: a comparison of three computer-assisted techniques. Magn Reson Imaging 1996;14:495–505.
16. Jenkinson M, Smith S. A global optimisation method for robust affine registration of brain images. Med Image Anal 2001;5:143–156.
17. Neeman M, Freyer JP, Sillerud LO. A simple method for obtaining cross-term-free images for diffusion anisotropy studies in NMR microimaging. Magn Reson Med 1991; 21:138–143.
18. Basser PJ, Mattiello J, LeBihan D. Estimation of the effective self-diffusion tensor from the NMR spin echo. J Magn Reson B 1994;103:247–254.
19. Basser PJ, Pajevic S, Pierpaoli C, Duda J, Aldroubi A. In vivo fiber tractography using DT-MRI data. Magn Reson Med 2000;44:625–632.
20. Calamante F, Tournier JD, Jackson GD, Connelly A. Track-density imaging (TDI): super-resolution white matter imaging using whole-brain track-density mapping. Neuroimage 2010;53:1233–1243.
21. Tzourio-Mazoyer N, Landeau B, Papathanassiou D, et al. Automated Anatomical Labeling of activations in SPM using a macroscopic anatomical parcellation of the MNI MRI single-subject brain. Neuroimage 2002;15:273–289.
22. Gong G, Rosa-Neto P, Carbonell F, Chen ZJ, He Y, Evans AC. Age- and gender-related differences in the cortical anatomical network. J Neurosci 2009;29: 15684–15693.
23. Avants BB, Tustison NJ, Song G, Cook PA, Klein A, Gee JC. A reproducible evaluation of ANTs similarity metric performance in brain image registration. Neuroimage 2011;54:2033–2044.
24. Klein A, Andersson J, Ardekani BA, et al. Evaluation of 14 nonlinear deformation algorithms applied to human brain MRI registration. Neuroimage 2009;46:786–802.
25. Latora V, Marchiori M. Efficient behavior of small-world networks. Phys Rev Lett 2001;87:198701.
26. Wang J, Wang L, Zang Y, et al. Parcellation-dependent small-world brain functional networks: a resting-state fMRI study. Hum Brain Mapp 2009;30:1511–1523.
27. Zalesky A, Fornito A, Bullmore ET. Network-based statistic: identifying differences in brain networks. Neuroimage 2010;53:1197–1207.
28. Holm SA. Simple sequentially rejective multiple test procedure. Scand J Stat 1979;6:65–70.
29. Imai K, Keele L, Tingley D. A general approach to causal mediation analysis. Psychol Methods 2010;15:309–334.
30. Park HJ, Kim JJ, Lee SK, et al. Corpus callosal connection mapping using cortical gray matter parcellation and DT-MRI. Hum Brain Mapp 2008;29:503–516.
31. Charlton RA, Morris RG, Nitkunan A, Markus HS. The cognitive profiles of CADASIL and sporadic small vessel disease. Neurology 2006;66:1523–1526.
32. Wen W, Zhu W, He Y, et al. Discrete neuroanatomical networks are associated with specific cognitive abilities in old age. J Neurosci 2011;31:1204–1212.
33. Nitkunan A. The use of quantitative magnetic resonance imaging techniques and neuropsychological tests to study cerebral small vessel disease [PhD thesis]. London: St George's, University of London; 2007.
34. Johansen-Berg H, Behrens TEJ. Just pretty pictures? What diffusion tractography can add in clinical neuroscience. Curr Opin Neurol 2006;19:379–385.
35. Behrens TE, Woolrich MW, Jenkinson M, et al. Characterization and propagation of uncertainty in diffusion-weighted MR imaging. Magn Reson Med 2003;50: 1077–1088.
36. Caeyenberghs K, Leemans A, De Decker C, et al. Brain connectivity and postural control in young traumatic brain injury patients: a diffusion MRI based network analysis. Neuroimage Clin 2012;1:106–115.
37. Van Wijk BCM, Stam CJ, Daffertshofer A. Comparing brain networks of different size and connectivity density using graph theory. PLoS One 2010;5:e13701.
38. Zalesky A, Fornito A, Harding IH, et al. Whole-brain anatomical networks: does the choice of nodes matter? Neuroimage 2010;50:970–983.
39. Cammoun L, Gigandet X, Meskaldji D, et al. Mapping the human connectome at multiple scales with diffusion spectrum MRI. J Neurosci Methods 2012;203:386–397.
40. Fornito A, Zalesky A, Breakspear M. Graph analysis of the human connectome: promise, progress, and pitfalls. Neuroimage 2013;80:426–444.